NASA Technical Memorandum 101565

# Characterization of the Bending Stiffness of Large Space Structure Joints

K. Chauncey Wu

May 1989

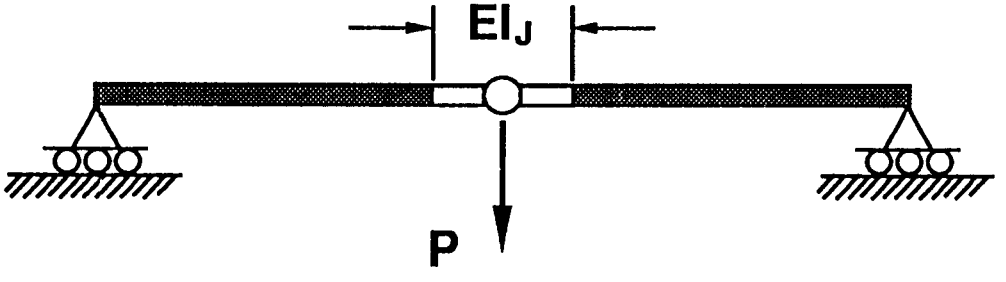




National Aeronautics and Space Administration

Langley Research Center
Hampton, Virginia 23665

# CHARACTERIZATION OF THE BENDING STIFFNESS OF LARGE SPACE STRUCTURE JOINTS

K. Chauncey Wu
NASA Langley Research Center
Hampton, VA 23665-5225

## INTRODUCTION

Extensive studies have been conducted to determine the axial stiffness characteristics of large space structure truss joints (references 1 and 2) because axial loading of the truss members dominates the structural response. However, the bending behavior of such truss joints is not understood as thoroughly. It is important to understand and quantify the bending stiffness of joints used in this class of structure, since the joint bending stiffness will have a strong influence on both the buckling load and natural frequency of individual truss members, as shown in reference 3. A conservative joint bending stiffness of zero may be assumed to estimate these values but the results may be misleading, since a relatively small joint bending stiffness can have a large effect on the behavior of the truss member. Past experience has shown that dynamic characterization of space trusses is extremely difficult if the member frequencies and truss frequencies are not widely separated (references 4 and 5). Based on this experience, it is desirable to have individual member frequencies which are higher than the fundamental frequencies of the complete truss structure. By quantifying the joint bending behavior, the truss member properties may be accurately predicted.

It is desirable for the truss joints in large space structures to have a linear axial load-deflection response. In order to accomplish this goal, the joint bending stiffnesses (EI) tend to be non-linear due to complicated internal mechanisms and load paths in the joint. It is difficult to use analytical methods exclusively to predict the joint bending stiffness because of this non-linear behavior. This paper presents a straightforward method of estimating the bending stiffness of truss joint concepts by using a combination of classical beam theory and experimental methods. This technique is demonstrated for a mechanically preloaded joint used in an experiment to evaluate the potential for automated assembly of large

space structures. Since this joint is to be used in a structurally redundant truss, the operational bending loads are expected to be small when compared to the axial loads. Consequently, characterizing the joint bending stiffness for applied bending moments of between 30 and 120 in-lbs is expected to cover the range of moments encountered in service.

## JOINT DESCRIPTION

The hardware used in this study is a mechanically preloaded, side-latching joint concept designed for automated structural assembly. The joint, shown in figures 1 and 2, is designed to provide a linear axial load-deflection response and eliminate any free play after assembly. The joint is assembled by inserting the connector into the receptacle (see figure 1) and given a compressive preload by applying a fixed torque to the locking nut, driving a wedge which pulls the connector and receptacle together and compresses a series of Belleville washers inside the joint (figure 2). The upper limit of the linear stiffness range under tensile loading is equal to the maximum compressive load in the Belleville washers. By loading the joint in tension, the compressive preload across the joint/receptacle interface is linearly reduced. After the preload is exceeded, the tensile load is taken up by the connector and transferred through the joint into the strut. When a compressive load is applied to the joint, the stresses at the interface contact surfaces are increased. Since these contact surfaces do not extend completely around the connector, the bending stiffness of this joint is likely to depend on the orientation of the joint symmetry plane with respect to the applied loading. A joint was bonded to each end of a 68.7 inch-long graphite/epoxy strut to form a complete truss member.

## ANALYSIS

To estimate the joint bending stiffness from experimentally measured deflections, an analysis of a beam with a variable cross-section loaded in three-point bending was performed (see figure 3). The derivation of a closed-form expression for the lateral deflection of the beam is shown in the appendix. The deflection at the beam mid-span ($x = L/2$) is:

$$y|_{x=L/2} = \frac{P}{EI_J}\left(\frac{L^3}{48} - \frac{a^3}{6}\right) + \frac{Pa^3}{6EI_S} \qquad (1)$$

In equation 1, the lateral deflection of the beam is y, the axial position along the beam is x and the applied mid-span load is P. L is the distance between the supports (81.4 in) and a is the distance from the support to the joint/strut interface (35.7 in). The bending stiffness of the graphite/epoxy strut is $EI_S$ and $EI_J$ is the effective bending stiffness of the two joints and the node. All of the terms in equation 1 are known or experimentally determined constants with the exception of the joint bending stiffness. Thus, equation 1 may be rearranged to yield:

$$EI_J = \left(\frac{L^3}{48} - \frac{a^3}{6}\right) \div \left(\frac{y|_{x=L/2}}{P} - \frac{a^3}{6EI_S}\right) \qquad (2)$$

It should be noted that this analysis is based on linear beam bending theory. Consequently, the term $y/P$ in equation 2 can be determined from the slope of the experimental mid-span load-deflection curve. In addition to the boundary conditions shown in figure 3, other assumptions inherent in this analysis are that the beam is symmetric with respect to its mid-span and that the applied loading passes through the shear center of the joint cross-section, preventing axial twist in the beam.

## JOINT BENDING TEST

A three-point bending test, shown in figure 4, was conducted to determine the experimental load-deflection response at the beam mid-span. The beam was comprised of two complete truss members connected to a node cluster and supported at each end with a fixture (see inset, figure 4) which permitted free rotation of the beam end. The mechanical joints were attached to receptacles which were bolted to the node at a given orientation. The preload in both joints was set to the same nominal value by applying a 20 in-lb torque to the locking nut. Incremental static loads of 1.56, 3.56 and 5.56 lbs (corresponding to mid-span moments of 31.7, 72.4 and 113.1 in-lbs, or $PL/4$) were applied at the node cluster. The resulting deflections of the node were measured with respect to its initial position with a mechanical dial gage. The bending stiffness of the

graphite/epoxy struts ($EI_S$, experimentally determined from similar three-point bending tests) was found to be $4.862 \times 10^5$ lb-in$^2$.

The independent parameter in this experiment was chosen to be the orientation of the joint symmetry plane with respect to the applied loading axis, shown in figure 5. To take advantage of the plane of symmetry in the joint, only orientations between 0 and 180 degrees (inclusive) were studied. Seven joint orientations of 0, 35, 55, 90, 125, 145 and 180 degrees were selected. The joint orientations at 35, 55, 125 and 145 degrees were convenient because a pin on the receptacle could be aligned with the arms of a cruciform slot cut into the node faces. The test procedure described above was repeated at each of the seven different joint orientation angles.

The support fixtures used in this experiment differ from ideal pin-roller boundary conditions in several ways. The center of rotation of the fixture was not coincident with the beam's neutral axis. Consequently, rotation of the strut causes small axial and lateral deflections at the supports. Also, axial motion of the struts at the supports was unrestrained except by small axial forces generated between the strut and the support. The reaction force at the supports was distributed over a 3 inch section of the strut, rather than at a knife-edge, to prevent local damage to the graphite/epoxy material and deflections due to distortion of the strut cross-section. Use of these support fixtures should not adversely affect the results, since the forces at the ends of the beam contribute only a small amount to the total bending strain energy of the system.

In addition to the gravity load on the beam, there is a bending moment at each support caused by the weight of the portion of the truss member on the opposite side of the support from the node. The analytical procedure was used to determine the deformed shape of the beam with respect to an arbitrary reference, in this case, the beam displacement field due to the constant loads described above. Thus, the measured deflections resulted only from the applied loading. Also, since the bending stiffnesses of the two joints were assumed to be equal in the analysis, application of the experimental procedure would only determine the average stiffness of the two joints tested.

## RESULTS AND DISCUSSION

Load-deflection data was taken at the beam mid-span for three applied moments at each of the seven joint orientation angles studied. A representative plot of the beam mid-span deflection versus the applied load is shown in figure 6. The ratio of the mid-span deflection and the corresponding applied load (the secant slope) from the loading curve in figure 6 was used with equation 2 to compute the bending stiffness of the joint. The term $y/P$ in equation 2 is equal to the inverse of the secant slope of a load-deflection curve for a linear beam. This secant formulation is exact for small bending moments, where the secant and tangent slopes are equal (in the range where the joint stiffness is linear). However, for large moments, the tangent slope is a better value for computing the joint bending stiffness than the secant slope. In the non-linear range, the secant slope tends to be higher than the tangent, resulting in a higher (and less conservative) computed joint bending stiffness. Computation of the secant joint bending stiffness in this test is justified based on the small number of experimental data points taken and the the uncertainty involved in determining the tangent slope of the experimental load-deflection data. If the joint bending stiffness is linear, then the secant and tangent slopes are equal and the assumptions made in deriving equations 1 and 2 are valid. The test data obtained was repeatable when the beam was tested immediately after the joints were locked. As the load cycle was repeated, the bending stiffness decreased. This stiffness reduction occured because the joint preload was being relieved by the cyclic loading.

The computed bending stiffness of the joint (normalized by the strut bending stiffness) was plotted against the corresponding mid-span deflection for the joint orientations and applied loads studied in figure 7. The joint bending stiffness was found to vary significantly at a given joint orientation and to decrease as the applied moment was increased. The maximum bending stiffness was $0.844 \times 10^5$ lb-in$^2$ (17.4 percent of the strut stiffness) for an applied moment of 31.7 in-lbs and a joint orientation angle of 90 degrees. The minimum bending stiffness of $0.301 \times 10^5$ lb-in$^2$ (6.2 percent of the strut stiffness) occurred for an applied moment of 113.1 in-lb and a joint orientation angle of 180 degrees. The joint bending stiffness was consistently higher at three of the joint orientation angles (35, 55 and 90 degrees).

During application of the load to the beam, a gap was observed to form at the contact surface between the joint and receptacle. This gap first appeared when the tensile bending stress at the edge of the joint/receptacle interface exceeded the compressive stress caused by the joint preload. As the applied bending moment was increased, the compressive contact area of the interface was reduced, reducing the apparent stiffness of the joint. Because the contact area was shrinking, the moment arm from the connector shaft to the centroid of the compressive contact area was increasing. The higher joint bending stiffnesses observed at 35, 55 and 90 degrees occurred at these orientations because the centroidal moment arms were longer than the corresponding moment arms at the other orientations. The maximum preload generated in the Belleville washers also affected the apparent bending stiffness of the joint. Although the joints used in this study were preloaded to the same nominal value using a calibrated torque wrench, any differences between the individual joints were averaged when determining the joint bending stiffness.

The analytical procedure developed in the appendix treated the section of the beam containing the two joints and the node as having an effective bending stiffness distributed over its length. Use of this analysis for joints which are thought to have a high bending stiffness should yield accurate results. Since all of the deformation observed during the joint bending tests occurred at the joint/receptacle interface, modeling the joint as a torsional spring located at the interface and representing the other components as rigid links may give a more accurate estimate of the joint bending stiffness than the model used. Such a rigid link analysis would probably be more applicable to joint designs which have a low bending stiffness.

## CONCLUSIONS

In this study, a technique to estimate the bending stiffness of large space structure truss joints was developed. To demonstrate this technique, the bending stiffness of one erectable joint concept was studied for three applied bending moments at seven joint orientation angles. The joint bending stiffness was found to be non-linear and to vary significantly at a given joint orientation angle. The joint bending stiffness ranged between 6 percent of the strut bending stiffness for an

applied moment of 113 in-lb and 17 percent of the strut bending stiffness for a 32 in-lb moment (at orientations of 90 and 180 degrees, respectively). Because the joints are used in a structurally redundant truss, the bending loads in the truss members are much smaller than their axial loads. Consequently, it is expected that the bending loads that the joints will encounter in service are within the range of applied loading studied here. The bending stiffness of a space truss joint will be highly dependent on the design of the particular joint concept. With this in mind, the techniques developed in this study may serve as a guide for determining the bending stiffness of other joint designs.

## REFERENCES

1. Schneider, M. E. and Keinholz, D. A.: Characterization of Joints Using the Force-State Mapping Technique, CSA Engineering Technical Report No. 85-12-02, December 1985

2. Keinholz, D. A. and Allen, B. R.: Force-State Testing of a Quick-Connect Joint, CSA Engineering Technical Report No. 87-02-01, February 1987

3. Razzaq, Z.; et al.: Stability, Vibration and Passive Damping of Partially Restrained Imperfect Columns, NASA TM 85697, October 1983

4. Pappa, R. S. and Juang, J. N.: Some Experiences with the Eigensystem Realization Algorithm, Sound and Vibration, January 1988

5. Warnaar, D. B. and McGowan, P. E.: Effects of Local Vibrations on the Dynamics of Space Truss Structures, Published in the proceedings of AIAA/ASME/ASCE/AHS 28th Structures, Structural Dynamics and Materials Conference and AIAA Dynamics Specialist Conference, Monterey, CA, April 6-8, 1987, Paper No. AIAA 87-0941

## APPENDIX

The derivation of an expression for the lateral deflection of a discontinuous cross-section beam in three-point bending is shown below. Additional information is given in figure 3.

$$\frac{d^2y}{dx^2} = \frac{M(x)}{EI(x)}$$

$$= \frac{(-P/2)x}{EI(x)}$$

$$= \frac{-Px}{2EI(x)}$$

$$\frac{dy}{dx} = \frac{-Px^2}{4EI(x)} + C_i$$

solve for $0 \le x \le a$

$$\frac{dy}{dx} = \frac{-Px^2}{4EI_S} + C_1 \qquad (A1)$$

solve for $a \le x \le L/2$

$$\frac{dy}{dx} = \frac{-Px^2}{4EI_J} + C_2 \qquad (A2)$$

find $C_2$ by solving at $x = L/2$

$$\left.\frac{dy}{dx}\right|_{x = L/2} = \frac{-P(L/2)^2}{4EI_J} + C_2 = 0$$

$$= \frac{-PL^2}{16EI_J} + C_2 = 0$$

$$C_2 = \frac{PL^2}{16EI_J} \qquad (A3)$$

equate slopes at x = a and solve for $C_1$

$$\left.\frac{dy}{dx}\right|_{x=a} = \frac{-Pa^2}{4EI_S} + C_1 = \frac{-Pa^2}{4EI_J} + \frac{PL^2}{16EI_J}$$

$$C_1 = \left(\frac{1}{EI_S} - \frac{1}{EI_J}\right)\frac{Pa^2}{4} + \frac{PL^2}{16EI_J} \qquad \text{(A4)}$$

substitute (A3) and (A4) into (A1) and (A2)

$$\frac{dy}{dx} = \frac{-Px^2}{4EI_S} + \left(\frac{1}{EI_S} - \frac{1}{EI_J}\right)\frac{Pa^2}{4} + \frac{PL^2}{16EI_J}, \quad 0 \le x \le a \qquad \text{(A5)}$$

$$= \frac{-Px^2}{4EI_J} + \frac{PL^2}{16EI_J}, \quad a \le x \le L/2 \qquad \text{(A6)}$$

integrating again,

$$y = \frac{-Px^3}{12EI_S} + \left(\frac{1}{EI_S} - \frac{1}{EI_J}\right)\frac{Pa^2x}{4} + \frac{PL^2x}{16EI_J} + C_3, \quad 0 \le x \le a \qquad \text{(A7)}$$

$$= \frac{-Px^3}{12EI_J} + \frac{PL^2x}{16EI_J} + C_4, \quad a \le x \le L/2 \qquad \text{(A8)}$$

solve for $C_3$ at x = 0

$$y|_{x=0} = 0 + 0 + 0 + C_3 = 0;\ C_3 = 0 \qquad \text{(A9)}$$

equate deflections at x = a to find $C_4$

$$y|_{x=a} = \frac{-Pa^3}{12EI_S} + \left(\frac{1}{EI_S} - \frac{1}{EI_J}\right)\frac{Pa^3}{4} + \frac{PaL^2}{16EI_J}$$

$$= \frac{-Pa^3}{12EI_J} + \frac{PaL^2}{16EI_J} + C_4$$

$$C_4 = \left(\frac{1}{EI_S} - \frac{1}{EI_J}\right)\frac{Pa^3}{4} + \left(\frac{1}{EI_J} - \frac{1}{EI_S}\right)\frac{Pa^3}{12}$$

$$C_4 = \left(\frac{1}{EI_S} - \frac{1}{EI_J}\right)\frac{Pa^3}{6} \qquad \text{(A10)}$$

substitute (A9) and (A10) into (A7) and (A8)

$$y = \frac{-Px^3}{12EI_S} + \left(\frac{1}{EI_S} - \frac{1}{EI_J}\right)\frac{Pa^2x}{4} + \frac{PL^2x}{16EI_J}, \quad 0 \le x \le a \qquad \text{(A11)}$$

$$= \frac{-Px^3}{12EI_J} + \frac{PL^2x}{16EI_J} + \left(\frac{1}{EI_S} - \frac{1}{EI_J}\right)\frac{Pa^3}{6}, \quad a \le x \le L/2 \qquad \text{(A12)}$$

solving (A12) at $x = L/2$,

$$y|_{x=L/2} = \frac{-P(L/2)^3}{12EI_J} + \frac{PL^2(L/2)}{16EI_J} + \left(\frac{1}{EI_S} - \frac{1}{EI_J}\right)\frac{Pa^3}{6}$$

$$= \frac{-PL^3}{96EI_J} + \frac{PL^3}{32EI_J} + \left(\frac{1}{EI_S} - \frac{1}{EI_J}\right)\frac{Pa^3}{6}$$

$$= \frac{P}{EI_J}\left(\frac{L^3}{48} - \frac{a^3}{6}\right) + \frac{Pa^3}{6EI_S} \qquad \text{(A13)}$$

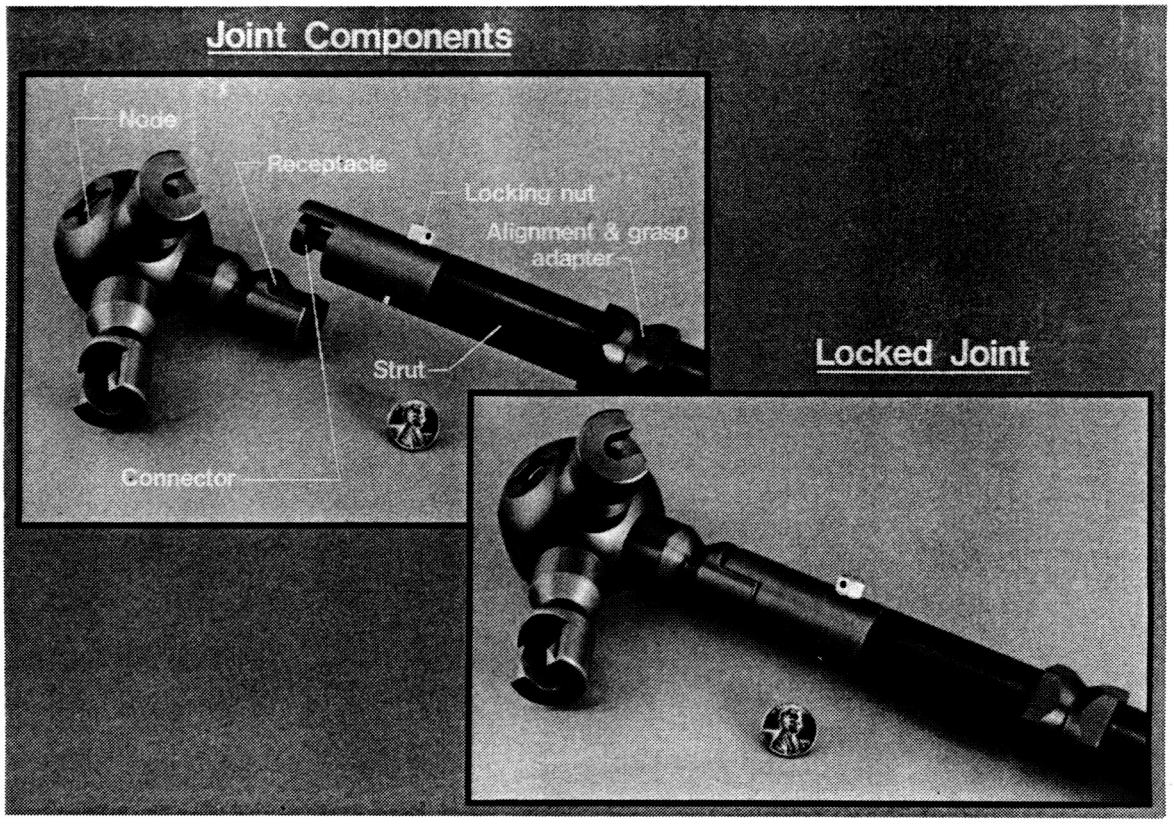


Figure 1: Mechanically Preloaded Joint

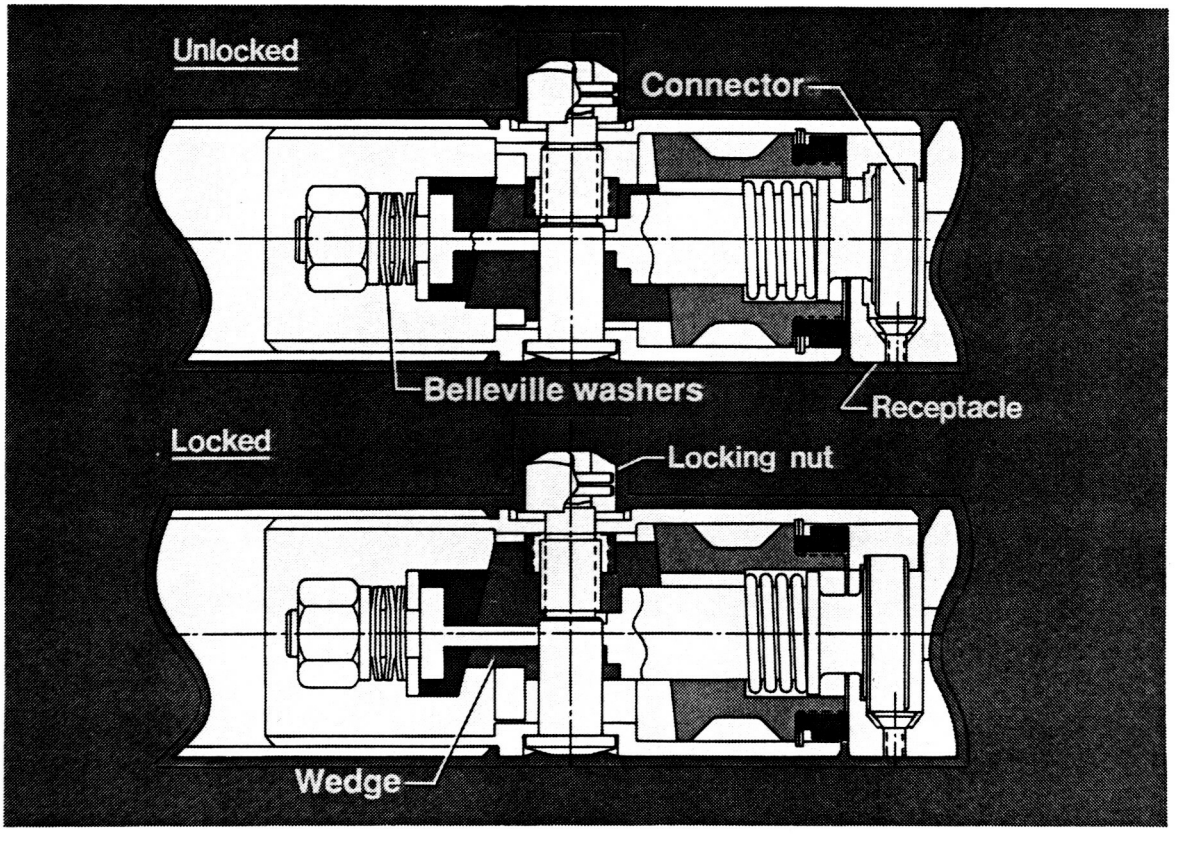


Figure 2: Joint Internal Mechanism

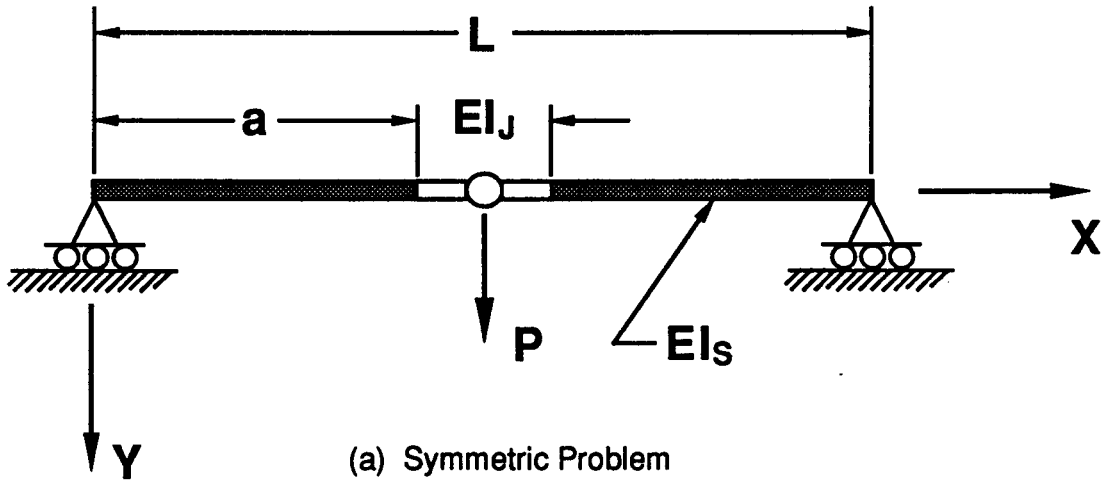


(a) Symmetric Problem

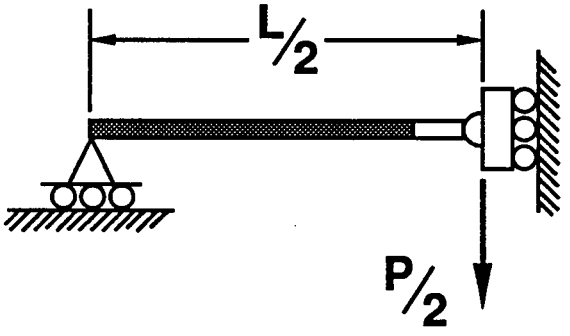


**Boundary Conditions**

$y = 0$ at $x = 0$

$\frac{dy}{dx} = 0$ at $x = L/2$

Continuity of Slope and Deflection at $x = a$

(b) Reduced Problem and Boundary Conditions

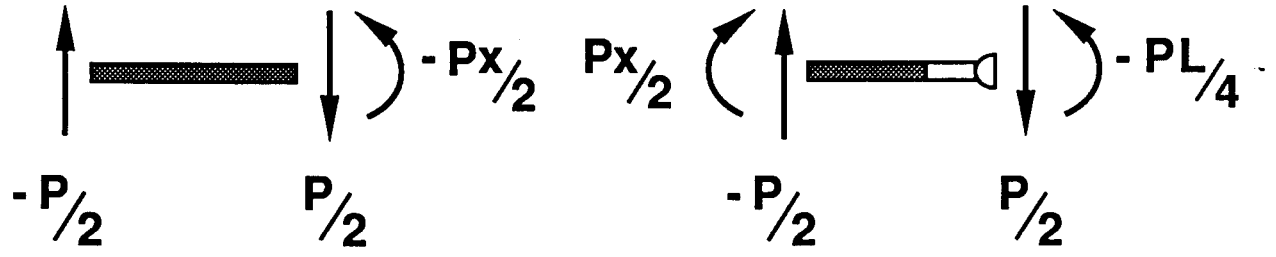


(c) Free-Body Diagrams

Figure 3: Analysis Schematic for a Discontinuous Cross-Section Beam in Three-Point Bending

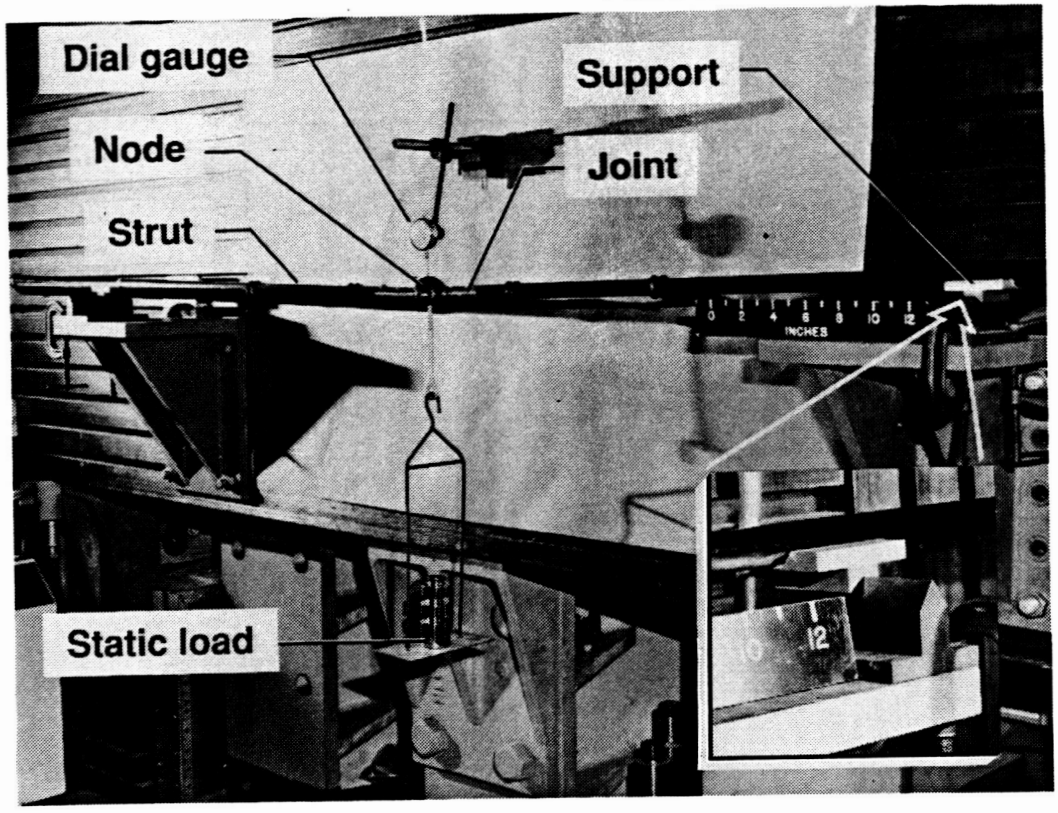


Figure 4: Three-Point Bending Test

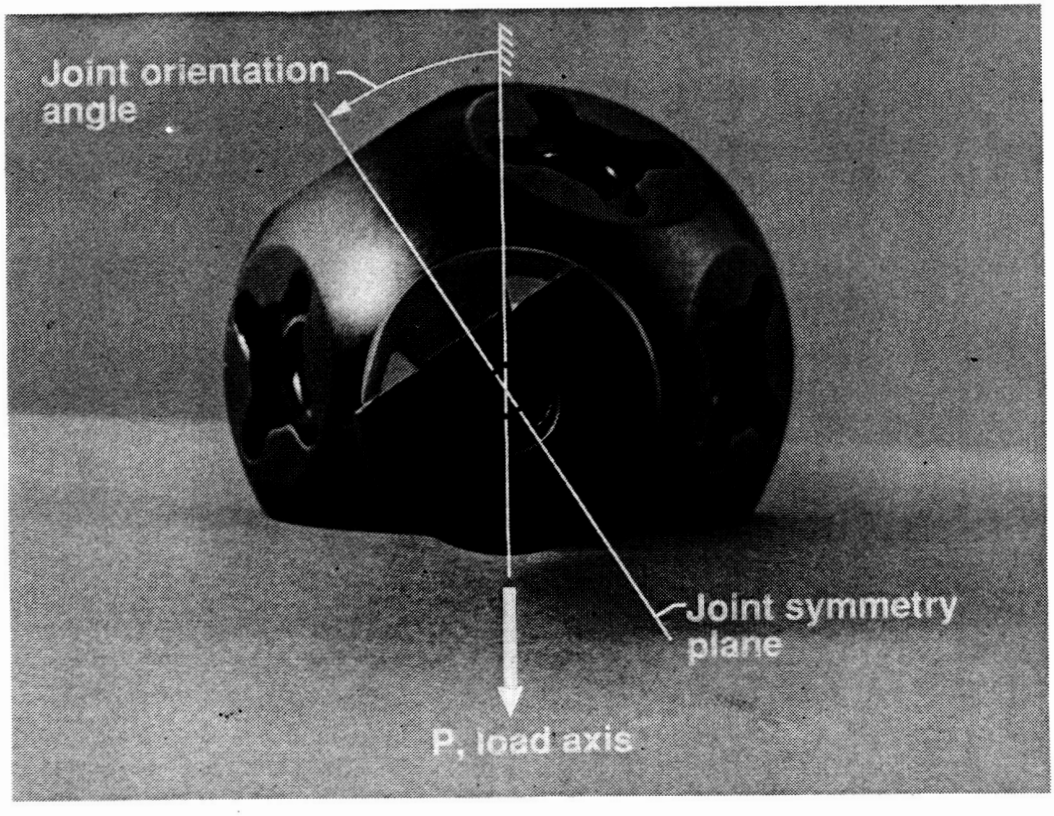


Figure 5: Joint Orientation Angle

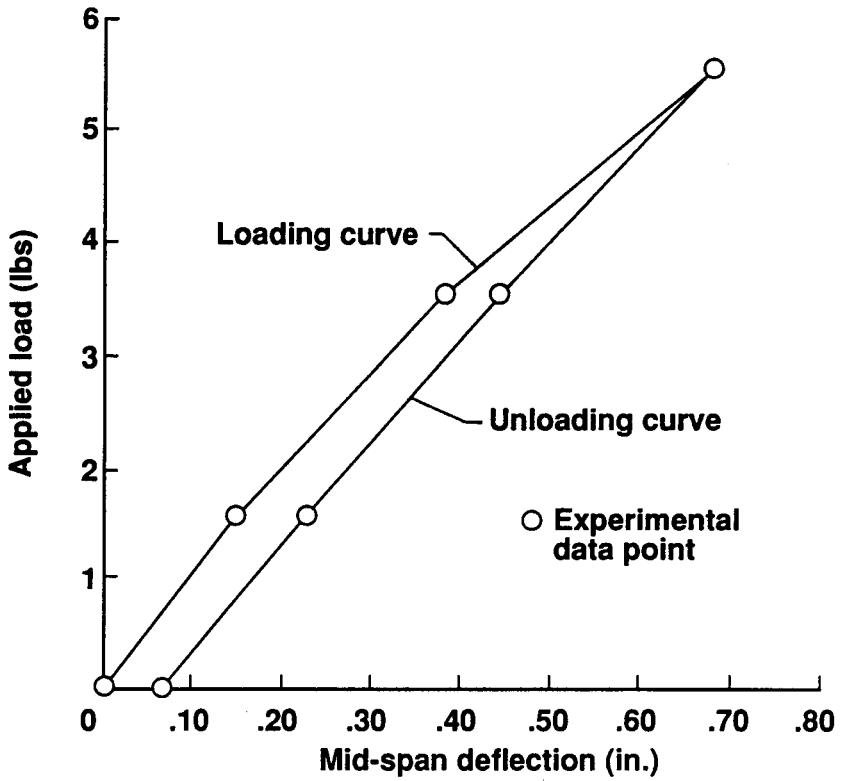


Figure 6: Mid-Span Load-Deflection Response
Joint Orientation Angle = 180 degrees

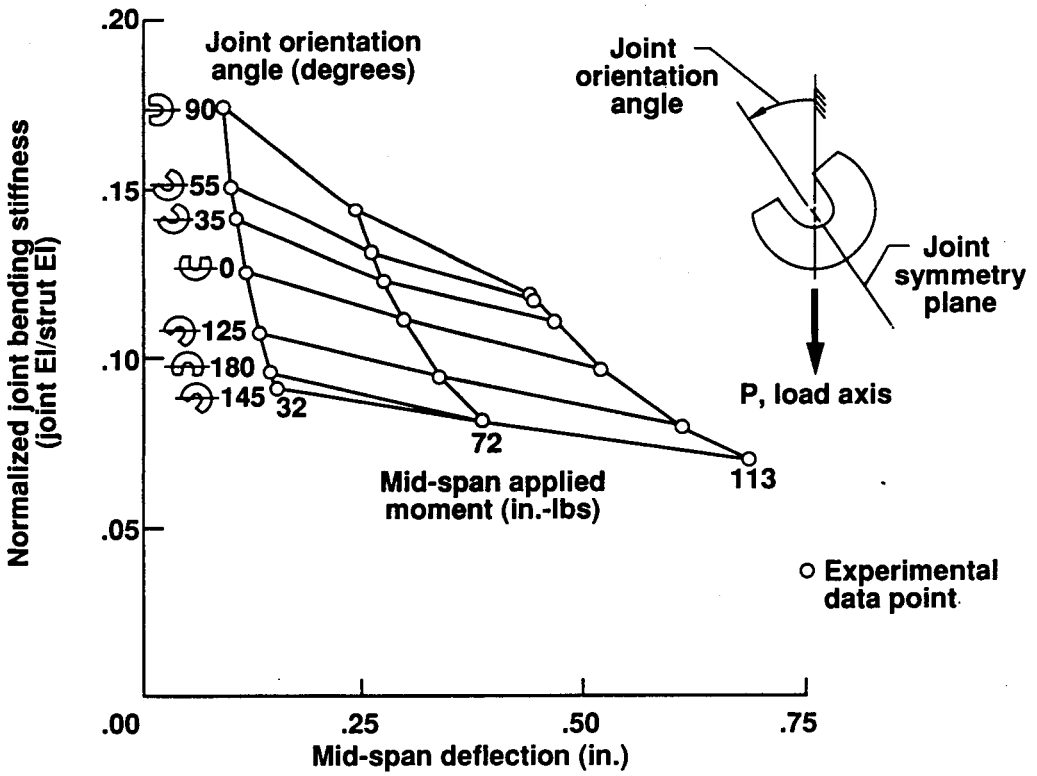


Figure 7: Normalized Joint Bending Stiffness

NASA
National Aeronautics and Space Administration

# Report Documentation Page

| 1. Report No. | 2. Government Accession No. | 3. Recipient's Catalog No. |
|---|---|---|
| NASA TM-101565 | | |

| 4. Title and Subtitle | 5. Report Date |
|---|---|
| Characterization of the Bending Stiffness of Large Space Structure Joints | May 1989 |
| | 6. Performing Organization Code |

| 7. Author(s) | 8. Performing Organization Report No. |
|---|---|
| K. Chauncey Wu | |
| | 10. Work Unit No. 506-43-41-02 |

| 9. Performing Organization Name and Address | 11. Contract or Grant No. |
|---|---|
| NASA Langley Research Center<br>Hampton, VA 23665-5225 | |
| | 13. Type of Report and Period Covered: Technical Memorandum |

| 12. Sponsoring Agency Name and Address | 14. Sponsoring Agency Code |
|---|---|
| National Aeronautics and Space Administration<br>Washington, DC 20546-0001 | |

15. Supplementary Notes


16. Abstract

A technique for estimating the bending stiffness of large space structure joints is developed and demonstrated for an erectable joint concept. Experimental load-deflection data from a three-point bending test is used as input to solve a closed-form expression for the joint bending stiffness which was derived from linear beam theory. Potential error sources in both the experimental and analytical procedures are identified and discussed. The bending stiffness of a mechanically preloaded erectable joint is studied at three applied moments and seven joint orientations. Using this technique, the joint bending stiffness was bounded between 6 and 17 percent of the bending stiffness of the graphite/epoxy strut member.


| 17. Key Words (Suggested by Author(s)) | 18. Distribution Statement |
|---|---|
| Large space structures<br>Joint bending stiffness<br>Truss member end fixity | Unclassified - Unlimited<br><br>Subject Category - 39 |

| 19. Security Classif. (of this report) | 20. Security Classif. (of this page) | 21. No. of pages | 22. Price |
|---|---|---|---|
| Unclassified | Unclassified | 16 | A03 |